

## Synthesis, structure and photoluminescence of two porous metal-organoboron frameworks with rtl topology

LIU Yan, XU Xin, XUAN WeiMin, ZHU ChengFeng & CUI Yong\*

State Key Laboratory of Metal Matrix Composites; School of Chemistry and Chemical Technology,  
Shanghai Jiao Tong University, Shanghai 200240, China

Received April 14, 2011; accepted May 19, 2011

Rigid trigonal tris(3-pyridyliduryl)borane **L** was synthesized through four steps in good overall yield from readily available 1,2,4,5-tetramethylbenzene and was used to construct two porous cadmium (II) complexes  $\text{Cd}(\mathbf{L})\text{X}_2 \cdot \text{G}$  ( $\text{X} = \text{Cl}, \text{Br}$ ;  $\text{G}$  = guest molecules), **1** ( $\text{Cd}(\mathbf{L})\text{Cl}_2 \cdot \text{EtOH} \cdot \text{iPrOH} \cdot 3\text{H}_2\text{O}$ ) and **2** ( $\text{Cd}(\mathbf{L})\text{Br}_2 \cdot \text{MeOH} \cdot \text{C}_7\text{H}_8 \cdot 3\text{H}_2\text{O}$ ), under mild reaction conditions. **1** and **2** are isostructural and featured with 3D porous metal-organoboron frameworks with rtl topology, in which **L** acts as a 3-connected node while a dicadmium motif serves as 6-connected node. In addition, **1** and **2** exhibit strong photoluminescence in the visible region and **1** shows moderate adsorption ability of carbon dioxide at 273 K.

**boron, metal-organic frameworks, coordination polymer, photoluminescence**

### 1 Introduction

Coordination-driven self-assembly method provides unique opportunities to design and prepare ordered arrays of molecules and clusters, and has led to significant progress in the Metal-organic frameworks (MOFs) [1, 2]. MOFs are attracting increasing attention not only because of their intriguing topologic structures but also due to their excellent properties and potential promising applications in catalysis, adsorption, separation, optics, magnetism and so on [3–7]. Pyridine-based ligands have been proved very useful building blocks to form 3D MOFs and numerous novel structures with fascinating properties have been constructed with this kind of ligands [8, 9]. On the other hand, three-coordinated boron, with its vacant p-orbital, is a useful  $\pi$ -acceptor in conjugated organic molecules [10, 11]. The inherently electron deficiency can lead to significant delocalization when conjugated with an adjacent organic  $\pi$ -system. Therefore, three-coordinated boron contained motifs are good candidates for construction of electrooptical and electronic mate-

rials [12, 13]. We have recently showed that rational combination of three-coordinated boron with pyridine-based coordination units will yield a  $C_3$ -symmetric tris(pyridyliduryl)borane that could be served as building block to fabricate a series of chiral octupolar NLO-active solids based on 3D coordination networks [14] and three porous networks exhibiting remarkable multiple (n,3) topology isomerism and excellent antibacterial activities and durability[15].

Encouraged by the successful construction of the aforementioned functional porous metal-organoboron frameworks and to further extend our work in this field, herein we design and synthesize a new  $C_3$ -symmetric tris(pyridyliduryl)borane ligand **L** and employ it to assemble with  $\text{CdCl}_2$  and  $\text{CdBr}_2$  to afford two isostructural porous metal-organoboron frameworks **1** and **2**. Photoluminescence and gas adsorption were studied to test their potential applications as optics and adsorbents.

### 2 Experimental

#### 2.1 Materials and apparatus

All of the chemicals were commercially available, and used

\*Corresponding author (email: yongcui@sjtu.edu.cn)

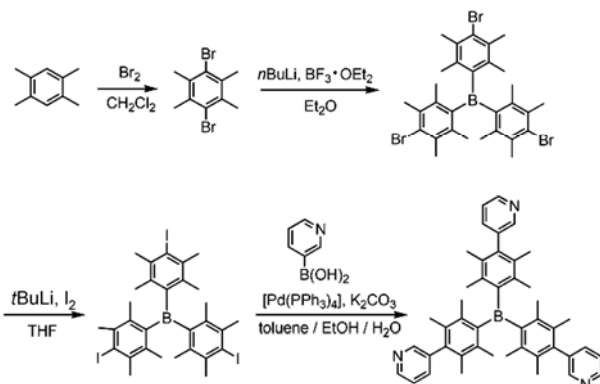
without further purification. Elemental analyses of C, H and N were performed with an EA1110 CHNS-O CE elemental analyzer. The IR (KBr pellet) spectra were recorded (400–4000 cm<sup>-1</sup> region) on a Nicolet Magna 750 FTIR spectrometer. Thermogravimetric analyses (TGA) were carried out in an N<sub>2</sub> atmosphere with a heating rate of 10 °C min<sup>-1</sup> on a STA449C integration thermal analyzer. The fluorescence spectra were carried out on an LS 50B Luminescence Spectrometer (Perkin Elmer, Inc., USA). High pressure adsorption measurements were carried out on a BELSORP-HP apparatus. The adsorption isotherm of CO<sub>2</sub> was measured using a volumetric adsorption system. Before the adsorption measurement, the sample was activated at 373 K under vacuum (<10<sup>-3</sup> torr) for 24 h.

## 2.2 Crystallographic measurements and structure determination

Single-crystal XRD data for the compounds was collected on a Bruker SMART Apex II CCD-based X-ray diffractometer with Mo-K $\alpha$  radiation ( $\lambda = 0.71073 \text{ \AA}$ ) for **1** and **2**. The two structures were solved by direct methods with SHELXS-97 and refined with SHEXLX-97 [16]. All the non-hydrogen atoms were refined by full-matrix techniques with anisotropic displacement parameters. The hydrogen atoms were geometrically fixed at calculated positions attached to their parent atoms, and treated as riding atoms. The crystallographic data and other pertinent information of complexes **1** and **2** are summarized in Table 1, and the selected bond lengths and bond angles are given in Table 2.

## 2.3 Synthesis of ligand

The ligand was synthesized in 75% yield by Suzuki coupling between 3-pyridylboronic acid and tris(iododuryl)-borane according to a reported procedure [14], which was obtained in three steps in good overall yield from readily available 1,2,4,5-tetramethylbenzene (Scheme 1). <sup>1</sup>H NMR (CDCl<sub>3</sub>)  $\delta$  (ppm): 8.59 (m, 3H), 8.41 (s, 3H), 7.49 (d, 3H), 7.37 (m, 3H), 2.08 (s, 18H), 1.85 (s, 18H).



Scheme 1 Synthesis of ligand **L**.

## 2.4 Synthesis of complex 1

The ligand (0.0032 g, 0.05 mmol), CdCl<sub>2</sub>·2.5H<sub>2</sub>O (0.034 g, 0.15 mmol), toluene (0.1 mL), <sup>i</sup>PrOH (0.5 mL) and EtOH (0.5 mL) were added to a small vial that was sealed and heated to 353 K for 3 d and then cooled to room tempera-

**Table 1** Crystal data for the title compound

Complex	1	2
Empirical formula	C49H66BCdCl2N3O5	C53H48BB2CdN3O4
Formula weight	971.16	1073.97
Radiation (MoK $\alpha$ ) (Å)	0.71073	0.71073
Crystal system, space group	monoclinic, $P2_1/c$	monoclinic, $P2_1/c$
$T$ (K)	293(2)	298(2)
$a$ (Å)	11.794(2)	12.125(9)
$b$ (Å)	25.683(5)	26.21(2)
$c$ (Å)	17.275(4)	17.467(1)
$\beta$ (°)	103.10(3)	104.727(1)
$V$ (Å <sup>3</sup> )	5096.5(2)	5369(7)
$Z$	4	4
$D_c$ (g cm <sup>-3</sup> )	1.266	1.938
$\mu$ (MoK $\alpha$ ) (cm <sup>-1</sup> )	0.578	1.194
F(000)	2032	2168
$\theta$ range for data collection (°)	3.09 to 25.00	1.55 to 25.00
Index ranges	$-12 \leq h \leq 14, -30 \leq k \leq 30, -20 \leq l \leq 20$	$-13 \leq h \leq 14, -22 \leq k \leq 31, -19 \leq l \leq 20$
Reflections collected/unique	38365/8915 ( $R_{\text{int}} = 0.0548$ )	24591/9216 ( $R_{\text{int}} = 0.0997$ )
Goodness-of-fit on $F^2$	1.023	0.918
$R$ , $wR$ ( $I > 2\sigma(I)$ )	$R_1 = 0.0642, wR_2 = 0.1698$	$R_1 = 0.0640, wR_2 = 0.1473$

**Table 2** Selected bond lengths ( $\text{\AA}$ ) and bond angles ( $^\circ$ )

Complex	<b>1</b>	Complex	<b>2</b>
Bond	Dist.	Bond	Dist.
Cd(1)-N(2)#1	2.353(5)	Br(1)-Cd	2.7579(17)
Cd(1)-N(3)#2	2.355(5)	Br(1)-Cd#1	2.7720(19)
Cd(1)-N(1)	2.411(4)	Br(2)-Cd	2.6939(16)
Cd(1)-Cl(2)	2.5761(15)	Cd-N(3)#2	2.375(6)
Cd(1)-Cl(1)	2.6187(16)	Cd-N(2)#3	2.381(7)
Cd(1)-Cl(1)#3	2.6405(15)	Cd-N(1)	2.437(6)
Cl(1)-Cd(1)#3	2.6405(15)	Cd-Br(1)#1	2.7720(19)
N(2)-Cd(1)#4	2.353(5)	N(2)-Cd#3	2.381(7)
N(3)-Cd(1)#2	2.355(5)	N(3)-Cd#4	2.375(6)
Angle	( $^\circ$ )	Angle	( $^\circ$ )
N(2)#1-Cd(1)-N(3)#2	174.43(17)	Cd-Br(1)-Cd#1	92.33(6)
N(2)#1-Cd(1)-N(1)	93.28(16)	N(3)#2-Cd-N(2)#3	176.2(2)
N(3)#2-Cd(1)-N(1)	87.02(16)	N(3)#2-Cd-N(1)	91.2(2)
N(2)#1-Cd(1)-Cl(2)	88.11(12)	N(2)#3-Cd-N(1)	86.7(2)
N(3)#2-Cd(1)-Cl(2)	86.32(13)	N(3)#2-Cd-Br(2)	89.64(17)
N(1)-Cd(1)-Cl(2)	94.71(12)	N(2)#3-Cd-Br(2)	87.43(18)
N(2)#1-Cd(1)-Cl(1)	89.68(12)	N(1)-Cd-Br(2)	95.30(16)
N(3)#2-Cd(1)-Cl(1)	90.71(12)	N(3)#2-Cd-Br(1)	92.81(17)
N(1)-Cd(1)-Cl(1)	172.44(12)	N(2)#3-Cd-Br(1)	90.21(18)
Cl(2)-Cd(1)-Cl(1)	92.34(5)	N(1)-Cd-Br(1)	86.62(16)
N(2)#1-Cd(1)-Cl(1)#3	89.89(12)	Br(2)-Cd-Br(1)	176.86(4)
N(3)#2-Cd(1)-Cl(1)#3	95.67(13)	N(3)#2-Cd-Br(1)#1	90.88(15)
N(1)-Cd(1)-Cl(1)#3	85.07(11)	N(2)#3-Cd-Br(1)#1	91.52(16)
Cl(2)-Cd(1)-Cl(1)#3	177.98(5)	N(1)-Cd-Br(1)#1	174.02(16)
Cl(1)-Cd(1)-Cl(1)#3	87.99(5)	Br(2)-Cd-Br(1)#1	90.33(6)
Cd(1)-Cl(1)-Cd(1)#3	92.01(5)	Br(1)-Cd-Br(1)#1	87.67(6)

Symmetry transformations used to generate equivalent atoms for **1**: #1  $x, -y+1/2, z-1/2$ ; #2  $-x+1, -y, -z+2$ ; #3  $-x, -y, -z+1$ ; #4  $x, -y+1/2, z+1/2$ .

Symmetry transformations used to generate equivalent atoms for **2**: #1  $-x+1, -y+1, -z$ ; #2  $x, -y+3/2, z-1/2$ ; #3  $-x+2, -y+1, -z+1$ ; #4  $x, -y+3/2, z+1/2$ .

ture. Colorless block-like crystals of **1** were obtained and the yield based on Cd salt is up to 78.3%. Anal. calcd (%) for  $\text{C}_{49}\text{H}_{66}\text{BCdCl}_2\text{N}_3\text{O}_5$ : C, 60.60; H, 6.85; N, 4.33. Found: C, 60.26; H, 6.82; N, 4.26. IR (KBr,  $\text{cm}^{-1}$ ): 3419 (s), 2923 (m), 2367 (w), 1575 (w), 1478 (w), 1417 (m), 1396 (m), 1301 (w), 1267 (s), 1193 (m), 1032 (w), 952 (s), 800 (w), 717 (s), 642 (m).

## 2.5 Synthesis of complex 2

The ligand (0.0032 g, 0.05 mmol),  $\text{CdBr}_2 \cdot 4\text{H}_2\text{O}$  (0.052 g, 0.15 mmol), toluene (0.1 mL), MeOH (0.5 mL), EtOH (0.5 mL) and DMSO (0.1 mL) were added to a small vial that was sealed and heated to 333 K for 12 h and then cooled to room temperature. Colorless block-like crystals of was obtained and the yield based on Cd salt is only 11.6%. Anal. calcd (%) for  $\text{C}_{53}\text{H}_{48}\text{BBr}_2\text{CdN}_3\text{O}_4$ : C, 59.27; H, 4.50; N, 3.91. Found: C, 58.96; H, 4.53; N, 4.02. IR(KBr,  $\text{cm}^{-1}$ ): 3422 (m), 2890 (w), 1624 (m), 1560 (m), 1542 (m), 1478 (s), 1458 (m), 1418 (s), 1394 (s), 1298 (w), 1262 (s), 1192 (m), 1090 (w), 1050 (w), 1030 (m), 950 (s), 850 (m), 798 (m), 752 (w), 716 (s), 640 (m).

## 3 Results and discussion

### 3.1 Synthesis and characterization

Two Cadmium (II) Complex complexes, **1** and **2**, were synthesized under mild reaction conditions. The bulk product of them was obtained by repeating the experiment and the resulting crystals were collected by filtration, washed several times with MeOH, and dried under vacuum for 2 h. The phase purity of the bulk samples of them was established by comparison of their observed and simulated X-ray powder diffraction patterns (Figure 1).

The thermal stability of **1** and **2** was investigated on crystalline samples under a  $\text{N}_2$  atmosphere from 40 to 700  $^\circ\text{C}$ . TGA result analysis of complex **1** shows that an initial weight loss of 10.78% from 40 to 66  $^\circ\text{C}$  is probably due to trapped guest alcohol (EtOH and  $i\text{PrOH}$ ) molecules (calculated 10.9%). When the temperature reaches 140  $^\circ\text{C}$ , the residual guest water molecules almost completely disappear with a further weight loss of 5.45% (calcd 5.56%). The weight loss of 7.35% in the range of 140 to 365  $^\circ\text{C}$  is corresponding to the loss of two coordinated chlorine atoms (calculated 7.45%). From then on, its framework starts to decompose. The MeOH and water guest molecules residing

in complex **2** completely disappear around 145 °C and the toluene molecules in **2** may be removed in the process of washing and collection. The weight loss of 12.96% in the range of 145 to 383 °C is corresponding to the loss of two coordinated bromide atoms (calcd 13.11%), after which, its framework starts to decompose (Figure 2).

### 3.2 Structural description

Single-crystal structure analysis reveals that **1** crystallizes in the monoclinic space group  $P2(1)/c$  with  $Z = 4$  and exhibits a 3D framework. As shown in Figure 3, the basic building unit of complex **1** contains one  $\text{Cd}(\text{L})\text{Cl}_2$  unit, one  $^i\text{PrOH}$ , one  $\text{EtOH}$  and three  $\text{H}_2\text{O}$  guest molecules. The coordination environment of the central boron atom of each **L** is completely trigonal planar with three duryl groups arranged in a propellerlike fashion. The dihedral angles between the boron planes and the duryl planes are from 52.36° to 58.81°, and those between the duryl planes and the outer pyridyl planes are from 63.43° to 83.75°. Each Cd center adopts a distorted octahedron by coordinating to three pyridine

groups from three **L** ligands and three halogen atoms, two of which(Cl1) bridge two cadmium atoms to form a binuclear  $\text{Cd}_2\text{Cl}_2$  unit (Figure 4). The bond angles around the Cd(1) atom range from 86.32(2) to 177.98(5)°, and the Cd(1)-N and Cd-Cl bond lengths in the range of 2.353(5) and 2.641(2) Å, respectively. Rectangular binuclear  $\text{Cd}_2\text{Cl}_2$  unit is almost coplanar, in which the bond angles of  $\text{Cl}1\text{-Cd}1\text{-Cl}1$ (87.99°) and  $\text{Cd}1\text{-Cl}1\text{-Cd}1$ (92.01°) are close to 90°, and the distance between the two non-bonded Cd atoms is 3.784(7) Å.

The dicadmium motif in **1** is linked to six ligands **L** and each **L** is linked to three dicadmium motifs to generate a 3D framework with a **rtl** topology. The topology of **1** can be described as a binodal  $(4.6^2)_2(4^2.6^{10}.8^3)$  net if the dicadmium motif is treated as a six-connected node and the ligand as a three-connected node (Figure 5). The network contains 1D channels with an opening of ~4.45 Å×2.1 Å along the *a*

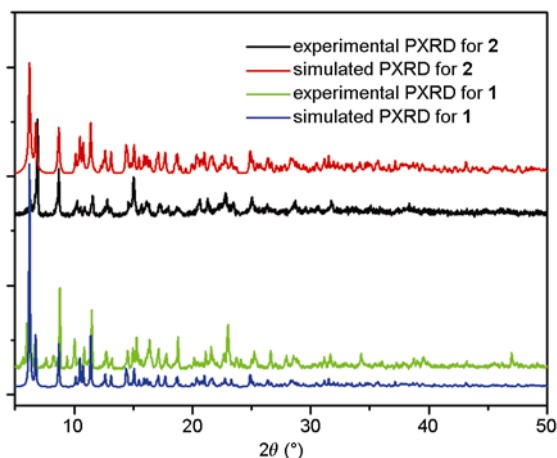


**Figure 1** Experimental and simulated powder XRD patterns of **1** and **2**, respectively.

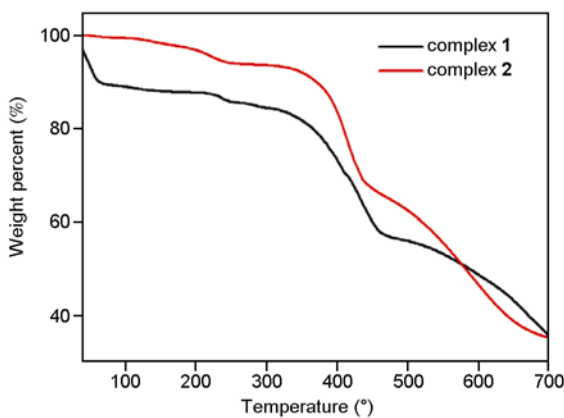


**Figure 2** Thermal analysis curves of the two cadmium complexes.

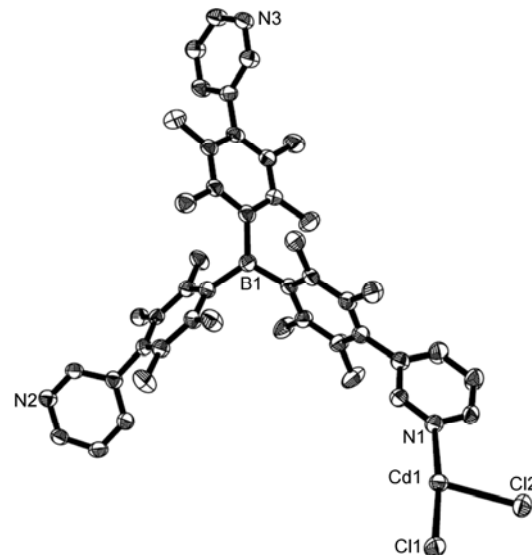


**Figure 3** Asymmetric unit of complex **1** (H atoms and guest molecules were omitted for clarity).

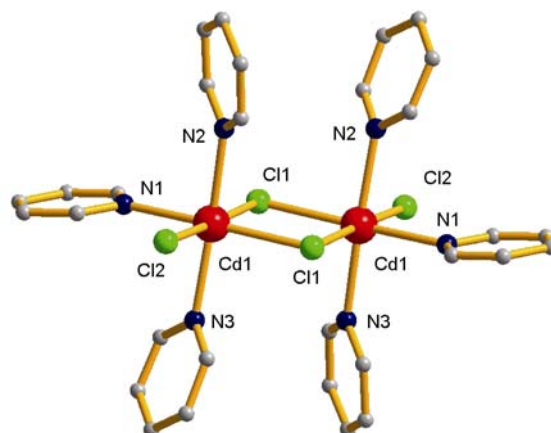


**Figure 4** Binuclear unit in **1**.

axis, suggesting potential adsorption and separation of gases with small kinetic diameter such as hydrogen, methane and carbon dioxide. The volume occupied by the lattice solvent molecules in **1** is  $1592\text{ \AA}^3$  per unit cell, which is 31.2% of the total crystal volume (calculated by the program PLATON [17]). High-pressure gas adsorption measurements were performed to investigate the  $\text{CO}_2$  uptake capacity of **1** (Figure 6). After activation at 100 °C under vacuum, **1** can take up 7.5 wt% ( $38\text{ cm}^3\text{ g}^{-1}$  STP) of  $\text{CO}_2$  at 20 bar and 273 K.

Single-crystal X-ray structure determination revealed that **2** is isostructural to **1**, but with different coordinated halogen atoms and guest molecules (one toluene, one MeOH and three water molecules). Besides this, there are also some minor differences in the corresponding bond lengths, bond angles and packing mode. The dihedral angles between the duryl planes and the boron plane range from 50.8° to 57.79° and that between the duryl planes and the outer phenyl planes is from 62.23° to 83.97°. Additionally, The bond angles around the Cd atom range from 86.62(2) to 176.86(4)°, and the Cd–N and Cd–Br bond lengths range from 2.375(6) and 2.7720(2) Å. More detailed data are presented in Table 2. Calculations with the PLATON program indicated that **2** has about 33.9% of total volume occupied by solvent molecules.

### 3.3 Photoluminescence property

Upon excitation at 320 nm, the emission spectra of **1** and

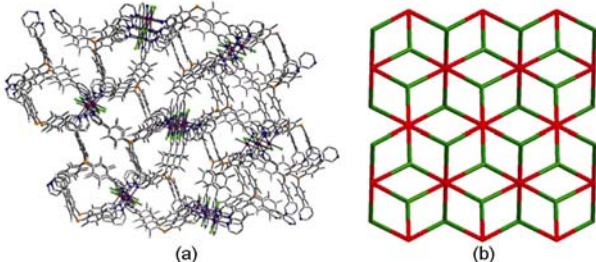


**Figure 5** (a) 3D structure of **1** along the *a* axis; (b) scheme showing the  $(4.6^2)_2(4^2.6^{10}.8^3)$  topology of **1**.

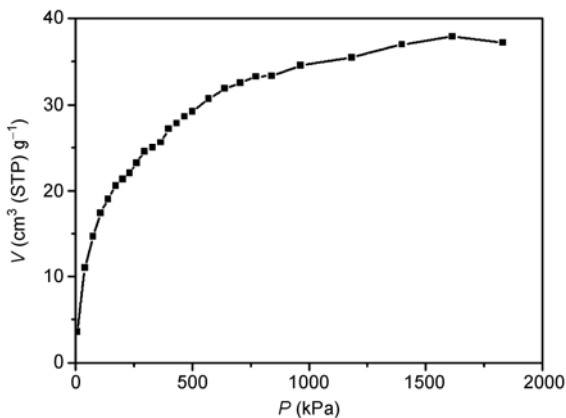


**Figure 6**  $\text{CO}_2$  adsorption isotherm of **1** measured at 273 K and 20 bar.

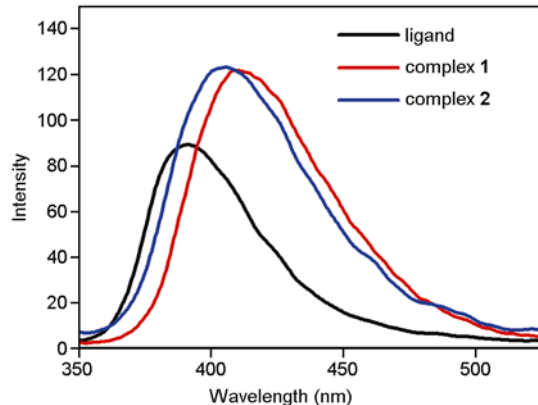


**Figure 7** Fluorescent emission spectra of **1**, **2** and **L**.

**2** are dominated by broad emission bands centered at 412 nm and 405 nm, respectively (Figure 7). Compared with the free ligand, the emissions of **1** and **2** show red-shift of about 20 and 14 nm, respectively. The slight difference for **1** and **2** may arise from the variation of halogen atoms, which is probably due to different coordination environments around the central metal ions caused by anions, because fluorescent behavior is closely related with the local chemical environments around metal centers [18]. All the emission peaks may be assigned to the ligand-centered  $\pi\rightarrow\pi^*$  or  $n\rightarrow\pi^*$  process.

### 4 Conclusions

In summary, we have synthesized two Cd-based porous metal-organoboron frameworks, **1** and **2**, from a rational designed  $C_3$ -symmetric tris(pyridyliduryl)borane multidentate ligands. **1** and **2** are isostructural and display **rtl** topology. As expected, the strong photoluminescence was found for **1** and **2** and can be tuned by the different coordinated halogen atoms. In addition, the porosity of **1** was verified by moderate uptake of carbon dioxide at 273 K.

This work was supported by the National Natural Foundation of China (21025103 & 20971085), the National Basic Research Program of China (2007CB209701 & 2009CB930403), and Shanghai Science and Technology Committee (10DJ1400100) and the Key Project of State Education Ministry.

- 1 Eddaoudi M, David BM, Li HL, Chen BL, Reineke TM, O'Keeffe M, Yaghi OM. Modular chemistry: Secondary building units as a basis for the design of highly porous and robust metal-organic carboxylate frameworks. *Acc Chem Res*, 2001, 34: 319–330
- 2 Qiu SL, Zhu GS. Molecular engineering for synthesizing novel structures of metal-organic frameworks with multifunctional properties. *Coord Chem Rev*, 2009, 293: 2891–2911
- 3 Lee JY, Farha OK, Roberts J, Scheidt KA, Nguyen ST, Hupp JT. Metal-organic framework materials as catalysts. *Chem Soc Rev*, 2009, 38: 1450–1459
- 4 Murray LJ, Dincă M, Long JR. Hydrogen storage in metal-organic frameworks. *Chem Soc Rev*, 2009, 38: 1294–1314

- 5 Li JR, Kuppler RJ, Zhou HC. Selective gas adsorption and separation in metal-organic frameworks. *Chem Soc Rev*, 2009, 38: 1477–1504
- 6 Allendorf MD, Bauer CA, Bhakta RK, Houk RJT. Luminescent metal-organic frameworks. *Chem Soc Rev*, 2009, 38: 1330–1352
- 7 Kurmoo M. Magnetic metal-organic frameworks. *Chem Soc Rev*, 2009, 38: 1353–1379
- 8 Evans OR, Lin WB. Crystal engineering of NLO materials based on metal-organic coordination networks. *Acc Chem Res*, 2002, 35: 511–522
- 9 Blake AJ, Champness NR, Hubberstey P, Li WS, Withersby MA, Schröder M. Inorganic crystal engineering using self-assembly of tailored building-blocks. *Coord Chem Rev*, 1999, 183: 117–138
- 10 Yamaguchi S, Akiyama S, Tamao K. Tri-9-anthrylborane and its derivatives: New boron-containing  $\pi$ -electron systems with divergently extended  $\pi$ -conjugation through boron. *J Am Chem Soc*, 2000, 122: 6335–6336
- 11 Yamaguchi S, Shirasaka T, Tamao K. Tridurylboranes extended by three arylethynyl groups as a new family of boron-based  $\pi$ -electron systems. *Org Lett*, 2000, 2, 4129–4132
- 12 Yamaguchi S, Shirasaka T, Akiyama S, Tamao K. Dibenzoborole-containing  $\pi$ -electron systems: Remarkable fluorescence change based on the “On/Off” Control of the  $p_{\pi}\text{--}\pi^*$  Conjugation. *J Am Chem Soc*, 2002, 124: 8816–8817
- 13 Wakamiya A, Mori K, Araki T, Yamaguchi S. A B-B bond-containing polycyclic  $\pi$ -electron system: Dithieno-1,2-dihydro-1,2-diborin and its dianion. *J Am Chem Soc*, 2009, 131: 10850–10851
- 14 Liu Y, Xu X, Zheng FK, Cui Y. Chiral octupolar metal-organoboron NLO frameworks with (14,3) topology. *Angew Chem Int Ed*, 2008, 47: 4538–4541
- 15 Liu Y, Xu X, Xia QC, Yuan GZ, He QZ, Cui Y. Multiple topological isomerism of three-connected networks in silver-based metal-organoboron frameworks. *Chem Commun*, 2010, 46: 2608–2610
- 16 Sheldrick GM. SHELXTL V5.1 Software Reference Manual, Bruker AXS, Inc., Madison, Wisconsin, USA, 1997
- 17 Spek AL. PLATON, Version 1.62, University of Utrecht, 1999
- 18 Wei KJ, Xie YS, Ni J, Zhang M, Liu QL. Syntheses, crystal structures, and photoluminescent properties of a series of M(II) coordination polymers containing M-X<sub>2</sub>-M bridges: From 1-D Chains to 2-D Networks. *Cryst Growth Des*, 2006, 6: 1341–1350